A new young stellar object in the S 187 complex : photometry and spectroscopy.

Annie Zavagno, Lise Deharveng, James Caplan

Astron. Astrophys. 281, 491–504 (1994)

ASTRONOMY
AND
ASTROPHYSICS

A new young stellar object in the S 187 complex: photometry and spectroscopy*

A. Zavagno, L. Deharveng, and J. Caplan

Observatoire de Marseille, 2 place Le Verrier, F-13248 Marseille Cedex 4, France

Received April 5, accepted July 26, 1993

Abstract. We report the discovery in the S 187 complex of a young stellar object with an optical counterpart. High resolution spectroscopy in the red and near infrared indicates that this object is a pre-main-sequence star. In the red, the spectrum is dominated by a very bright Hα line with a total width (wing to wing) greater than 1000 km s^{-1}. This line exhibits a special type of P Cygni profile (Beals's Type III). The object's near infrared spectrum is dominated by the Ca II triplet emission at 8498 Å, 8542 Å, and 8662 Å; these lines are broad and optically thick. Numerous Fe I and Fe II emission lines are observed also. B, V, R, I, H, K, and L magnitudes of the object, as well as its Hα luminosity, indicate that it is probably a Herbig late Be or early Ae star. It presents many characteristics of the "outflow group" of Herbig stars identified by Hamann & Persson (1992b); it is very similar, both in luminosity and geometry, to the well-known young stellar objects V645 Cyg and R Mon.

Key words: stars: pre-main-sequence – line: profiles – interstellar medium: individual objects: S 187

1. Introduction

Few massive young stellar objects (YSOs) are presently known (cf. the review by Henning 1990); among these are the BN objects which are not optically visible. However, a few very luminous YSOs such as V645 Cyg and R Mon have optical counterparts. Such objects are worth studying because they give information about the immediate vicinity of the star and its associated wind (geometry, velocity distribution, and physical conditions).

We have searched for new massive YSOs with red or near infrared counterparts. The candidates were high luminosity IRAS sources for which $L_{\rm IR} \geq 10^3\ L_{\odot}$ – the luminosity of a B3 main sequence star – and which are associated with CO outflows. The selected fields were observed at the 120 cm telescope of the Haute Provence Observatory, through V, R, I, and Hα filters. The detected objects were then observed spectroscopically.

We have discovered, in the S 187 complex, a stellar optical object with all the characteristics of a pre-main-sequence star, possibly a Herbig Ae/Be star. This object, which we call S 187Hα, was detected thanks to its strong Hα emission. Star formation seems active in the S 187 complex, as several distinct sites lie at the border of this H II region. The various components of the complex are described in Sect. 2. Photometric observations of the stellar field in the visible are presented in Sect. 3 along with photometric observations of the object in the near infrared; coordinates are given, as well as V, R, I, H, K, and L magnitudes. Spectroscopic observations of the object are presented and commented upon in Sect. 4. The extinction and spectral energy distribution of S 187Hα are discussed in Sect. 5. Our conclusions about the nature of S 187Hα are given in Sect. 6.

2. The H II region S 187 and its environment

The overall S 187 complex has been fully observed and discussed at large scale by Joncas et al. (1992) – hereafter JDR. S 187 (Sharpless 1959) is a small optical H II region located in the direction of the dark nebula L1317 (Lynds 1962). Its kinematical distance – the only one known[1] – is about 1 kpc (Fich & Blitz 1984); thus S 187 probably belongs to the Orion arm.

S 187 has often been observed in the radio continuum at low angular resolution, most recently by JDR. The observations of Israel (1977) and those of Snell & Bally (1986), obtained with higher angular resolution, allow one to separate the different radio sources. Figure 1 shows the VLA map obtained by Snell & Bally (1986) at 1.4 GHz (resolution 8.″3) projected on an R frame. S 187-1 (S 187A in Israel 1977), composed of two ultra-compact radio sources, has a non-thermal spectrum and is probably an extragalactic object. The nature of the compact source S 187-2 is unknown. The thermal source (S 187B in Israel 1977) is the extended object centered at $\alpha_{1950} = 1^{\rm h}19^{\rm m}50^{\rm s}$, $\delta_{1950} = +61°35'45''$, which corresponds well with the optical

Send offprint requests to: A. Zavagno

* Based on observations made at the Observatoire de Haute Provence

[1] Israel (1977) erroneously quotes Georgelin (1975) to justify a distance of 3 kpc for the exciting star.

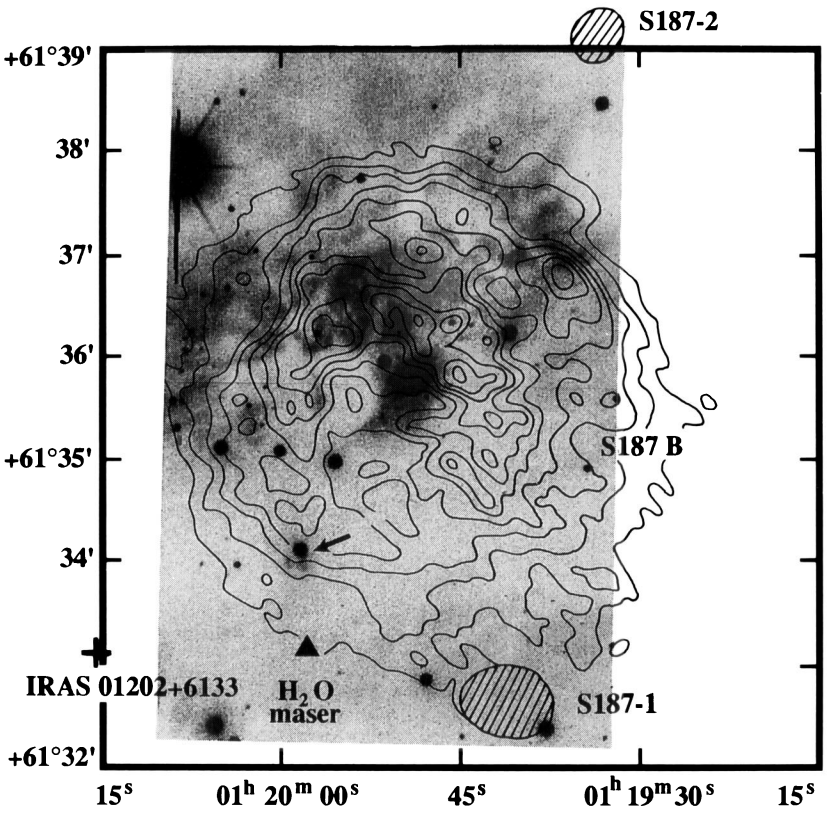

Fig. 1. The 1.4 GHz map obtained with the VLA by Snell & Bally (1986) is superimposed on an R frame of S 187. The cross marks the position of the near infrared source coincident with IRAS 01202+6133 and the triangle that of the H_2O maser discussed in the text. The arrow points to the pre-main-sequence object S 187Hα

nebula. This is a small (FWHM $\sim$ 1 pc) but somewhat evolved shell-like H II region, surrounding a cluster of bright stars. JDR estimate a maximum electron density of 100 cm^{-3} and, for the whole H II region, a mass of ionized gas of 7 $M_\odot$ and an excitation parameter of 13 pc cm^{-2}; this suggests an exciting star of spectral type B0.5. JDR show that the H II region is surrounded by a thick clumpy H I shell of about 70 $M_\odot$.

S 187 belongs to a large molecular complex. The CO emission has been mapped by Casoli et al. (1984a, 1984b) and by JDR. The molecular cloud (100′ north-south × 80′ east-west) lies some 15′ east of the H II region and its associated H I shell; its general aspect closely resembles that of the dark nebula L1317. The velocity structure of this cloud is complicated; Casoli et al. have interpreted it as the collision of two molecular clouds, which gives rise to gas compression and to star formation, producing the stellar cluster associated with S 187B and a few other objects discussed below.

Several sites of star formation lie in the direction of this complex.

A compact infrared source lies south-east of the H II region (cf. Fig. 1). It has been observed in the near infrared by Bally (quoted by Snell & Bally 1986), at $\alpha_{1950} = 1^h20^m15\overset{s}{.}2 \pm 0\overset{s}{.}7$ and $\delta_{1950} = +61°33'08'' \pm 5''$.This object corresponds to the bright infrared source IRAS 01202+6133, for which $L_{IR} \leq 2800\, L_\odot$ (Mozurkewich et al. 1986, after correcting the distance to 1 kpc). Two other IRAS sources lie nearby: IRAS 01203+6135 and IRAS 01195+6136. The former, a weak source, is detected at 12 μm and has no optical counterpart. IRAS 01195+6136 ($L_{IR} \approx 2400\, L_\odot$, Mozurkewich et al. 1986) is an extended source, centered on the H II region and possibly corresponding to associated dust emission. The infrared source AFGL 205 probably encompasses all these objects.

Bally & Lada (1983) searched for high velocity molecular material in the direction of IRAS 01202+6133. Two arcminutes west of the source, at $\alpha_{1950} = 1^h19^m58^s$, $\delta_{1950} = +61°33'08''$, they detected the high velocity CO source "S 187IRS" with a full width at 0.1 K of 30 km s^{-1}. This source has been mapped in ^{12}CO, with a resolution of 1′.4, by Casoli et al. (1984b) and Casoli (1986). Their map, presented in Fig. 2, clearly shows an extended bipolar CO outflow.

H_2O maser emission was later detected by Henkel et al. (1986) in the direction of this CO outflow. The velocity of this maser is close to the mean velocity of the associated molecular cloud (cf. Table 4). The maser lies between the blue and the red wings of the CO outflow. Thus this H_2O maser is associated with the molecular complex and the CO outflow.

The compact near-infrared source and the CO outflow (with the associated maser) are separated by about two arcminutes. We believe that this separation is real, as it is greater than the beam sizes of the instruments used for these observations. Furthermore, ammonia emission – a tracer of high density molecular gas – has been detected and mapped (Torrelles et al. 1986); it peaks in a third direction (Fig. 2), about 1.2 arcminutes north of the CO outflow and H_2O maser. This separation remains to be confirmed. Note that S 187Hα lies close to the NH_3 peak.

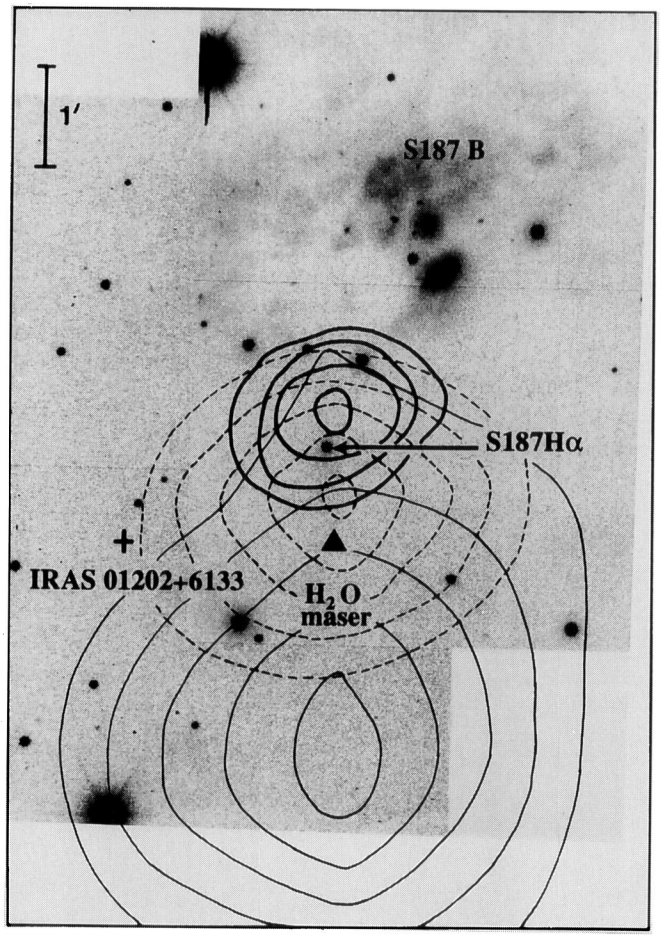

Fig. 2. The map of the CO outflow observed by Casoli et al. (1984b) (dashed lines for the blue wing, thin lines for the red wing), is superimposed on two V frames of the field. Ammonia emission (thick lines) was observed by Torrelles et al. (1986). The scale is the same as in Fig. 1

3. Photometry

V, R, I, and Hα frames of the S 187 region were obtained with the 120 cm telescope of the Observatoire de Haute Provence, on the night of 1990 September 20–21. The detector was an RCA CCD with 512 × 323 30-μm-square pixels. The scale at the F/6 Newtonian focus is 0.″85 per pixel and the seeing was 2.″2 (FWHM). We used V, R, and I filters approximating the Cousins (1976) system (the filter parameters are given by Chevalier & Ilovaisky 1991), and an Hα filter (FWHM 11 Å). Two frames (exposure times 50 s and 300 s) were obtained with each filter.

Figure 3 presents the V, R, I, and Hα frames. S 187B lies at the center; diffuse emission covers the northern part of the field. Absorption features are conspicuous in the eastern and southern parts of S 187B. In this area the molecular material and the associated dust are situated in front of the H II region. The newly detected Hα emission object S 187Hα (indicated by an arrow in Figs. 1, 2, and 3d) lies in the direction of the absorption feature. It is stellar in appearance; a small reflection nebula, whose axis may possibly be aligned with the CO outflow, lies to the south (Fig. 3 and 4a).

We used the DAOPHOT stellar photometry package (Stetson 1987) to reduce the CCD frames. The color equations established by Chevalier & Ilovaisky (1991) were used to transform the magnitudes in our photometric system to standard Cousins (1976) magnitudes and colors. The cluster NGC7790 (Christian et al. 1985), which lies close to S 187 in the sky, was observed several times during the night to correct for atmospheric extinction. This night was not of good photometric quality; however, as the observations of NGC7790 bracket those of S 187, the error is probably less than 0.1 mag both for magnitudes and colors. Table 1 gives the results obtained for 24 stars in the field. In the first column is the number corresponding to Fig. 3a. The next two columns give the right ascension and declination for the equinox 1950; these coordinates were obtained as explained in the Appendix. The fourth, fifth, and sixth columns give the magnitude V and the color indices $V-R$ and $V-I$ in the Cousins photometric system. JDR have obtained B, V, and R photometric measurements for some of these stars; the last four columns give JDR's identification numbers, and their V, $B-V$ and $V-R$. The two sets of measurements are in relatively good agreement; our $V-R$ colors are however slightly redder. JDR did not separate one close pair of bright stars – our nos. 12 and 13, their no. 7 (Fig. 4b).

S 187Hα, labelled no. 20, lies at $\alpha_{1950} = 1^{h}19^{m}58.^{s}37$, $\delta_{1950} = +61°34'04.''0$. This position corresponds neither to the strong near infrared source (some 2.2 arcmin away) nor to the center of the CO outflow and its associated H_2O maser (some 0.9 arcmin away), but rather to that of the NH_3 peak (Fig. 2).

The V versus $V-I$ diagram is presented in Fig. 5; we have drawn the main sequence assuming a distance of 1 kpc. The exciting star of the H II region S 187B is very probably no. 11 which, if situated at a distance of 1 kpc, would be a B1 V star with about 6.8 mag of visual extinction; this is consistent with the radio continuum emission of the H II region (see Sect. 2). S 187Hα – no. 20 – is one of the most reddened objects of the field. If this object were a main sequence star, its V and $B-V$ would indicate a spectral type B8 with a visual extinction of 6.1 mag, although its V and $V-I$ would suggest a B5 with an extinction of 6.9 mag. Stars 7, 10, 12, and 13 – which with star 11 form the bright cluster at the center of S 187B (Fig. 4b) – are probably B stars too, with extinctions ranging from 4 to 6 mag. A number of stars (1, 2, 3, 8, 18, 22, 23, 24) are seen in Fig. 5 to lie just above the main sequence; these are possibly foreground stars, located at about 800 pc, with little extinction. Alternatively, these stars may be located at about 1 kpc and thus be associated with the S 187 complex, but in that case they would be affected by a foreground extinction of the order of 1 mag.

S 187Hα was observed in H, K, and L by Sèvre & Arditti (private communication) at the 80 cm telescope of the Observatoire de Haute Provence in 1992 January and August, with

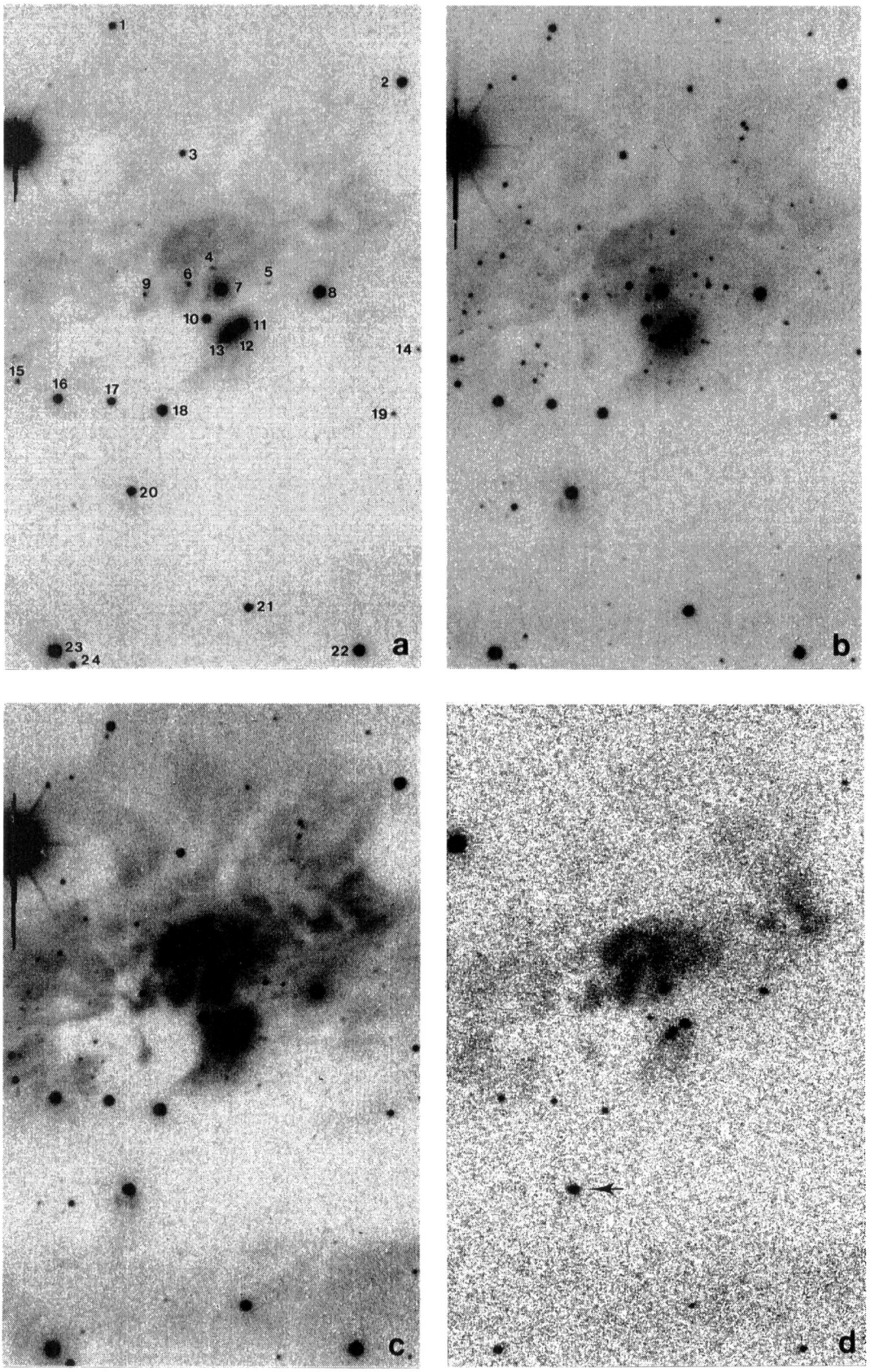

Fig. 3. a–d. V **a**, I **b**, R **c**, and Hα **d** frames obtained at the 120 cm telescope of the Observatoire de Haute Provence. S 187Hα appears as a bright Hα emission object (arrow in Fig. 3d). All the stars discussed in the text are identified by their numbers (Fig. 3a) from Table 1

Table 1. Coordinates and photometry of stars

No.	α_{1950}	δ_{1950}	V	$V-R$	$V-I$	JDR No.	V_{JDR}	$(B-V)_{JDR}$	$(V-R)_{JDR}$
1	$1^h\ 19^m\ 59.^s52$	$+61°\ 39'\ 05.''0$	17.21	0.77	1.47				
2	1 19 33.50	61 38 26.0	15.27	0.42	0.85				
3	1 19 53.31	61 37 42.0	17.68	0.84	1.60				
4	1 19 50.80	61 36 27.9	19.37	1.30	2.34				
5	1 19 45.76	61 36 17.5	19.78	0.98	2.57				
6	1 19 52.92	61 36 17.7	18.43	1.18	2.29				
7	1 19 50.03	61 36 13.4	13.74	0.71	1.48	4	13.64	1.24	0.60
8	1 19 41.14	61 36 11.4	13.86	0.34	0.71	3	13.81	0.85	0.36
9	1 19 56.89	61 36 11.0	18.95	1.18	2.54				
10	1 19 51.36	61 35 54.9	15.70	1.05	2.21	5	15.64	1.57	0.93
11	1 19 48.20	61 35 50.6	13.51	1.15	2.39	6	13.69	1.46	0.98
12	1 19 49.28	61 35 46.0	13.75	0.92	1.92	} 7[a]	14.61	1.46	0.85
13	1 19 49.60	61 35 42.7	14.64	0.90	1.97				
14	1 19 32.35	61 35 33.0	19.08	0.98	1.88				
15	1 20 08.54	61 35 15.7	18.56	1.14	2.31				
16	1 20 04.88	61 35 03.9	15.13	0.71	1.48	9	15.11	1.30	0.68
17	1 20 00.06	61 35 01.8	16.48	1.05	2.14				
18	1 19 55.48	61 34 55.4	14.67	0.39	0.81	10	14.64	0.97	0.43
19	1 19 34.70	61 34 51.4	19.07	1.10	2.20				
20[b]	1 19 58.37	61 34 04.0	15.82	1.28	2.56	11	15.90	1.78	1.24
21	1 19 47.95	61 32 47.0	16.27	1.26	2.62				
22	1 19 38.06	61 32 18.3	14.41	0.45	0.88				
23	1 20 05.44	61 32 20.4	13.36	0.33	0.72				
24	1 20 03.83	61 32 11.1	16.92	0.67	1.29				

[a] JDR do not separate the pair of bright stars Nos. 12 and 13
[b] S 187Hα

IRPHOT2. They obtained $H=10.2\pm0.5$, $K=8.7\ \pm\ 0.3$, and $L=4.9\ \pm\ 0.7$ with a diaphragm of 35 arcsec.

If S 187Hα were a main sequence star, its V and $V-K$ would correspond to a B1 star affected by some 8.7 mag of visual extinction. When comparing with the spectral types and extinctions derived from the optical magnitudes and colors, we see that S 187Hα cannot be a main sequence star. S 187Hα is more probably an object with a near infrared excess; we shall return to this point in Sect. 5.

4. Spectroscopy of S 187Hα

4.1. Observations and reductions

These observations were obtained with the CARELEC spectrograph at the 193 cm telescope of the Observatoire de Haute Provence. The detector was a Thomson CCD with 576 pixels in the direction of the dispersion and 384 pixels along the slit. Details of the observations are given in Table 2. Two main spectral ranges were observed – from 6320 Å to 6740 Å (hereafter the Hα range), and from 8380 Å to 8780 Å (the near infrared range). The exposure time was one hour for each spectrum. The 25° orientation of the slit (i.e. roughly NNW to SSE) allowed us to observe both the object and the H II region. The dispersion was 0.85 Å per 23 μm pixel in the Hα range and 1.1 Å per pixel in the near infrared range. Further technical details about the instrument can be found in Lemaître et al. (1990).

Table 2. Summary of spectroscopic observations

Wavelength	Date	Position angle	Slit width
Hα	1990 Oct 09	25° (NNW–SSE)	3.″3
Hα	1990 Nov 22	25°	3.″3
Hα	1992 Jan 28	25°	2.″8
Hα	1992 Jan 30	90° (E–W)	2.″8
near infrared	1990 Oct 11	25°	3.″3
near infrared	1990 Nov 21	26°	3.″3
near infrared	1992 Jan 31	90° (E–W)	2.″8
near infrared	1992 Feb 01	90° (E–W)	2.″8

We used the MIDAS environment for data reduction. The spectral resolution, defined as the FWHM of neon and argon arc emission lines, is about 80 km s^{-1} in the Hα range and 60 km s^{-1} in the near infrared range. The standard stars observed for the photometric calibration in the Hα range were Hiltner 102, Hiltner 600, and BD +28°4211 from Stones (1977); and Cyg OB2 No. 9 and Feige 34 from Massey et al. (1988). In the near infrared range we used W 1346 and 40 Eri B from Oke (1974); and HD 19445, HD 84937, and BD +26°2606 from Oke & Gunn (1983). The sensitivity as a function of wavelength was derived from the stellar observations; comparison of these curves give an estimate of the photometric accuracy, which is about ±4.5% near Hα and ±6.5% in the near infrared; this

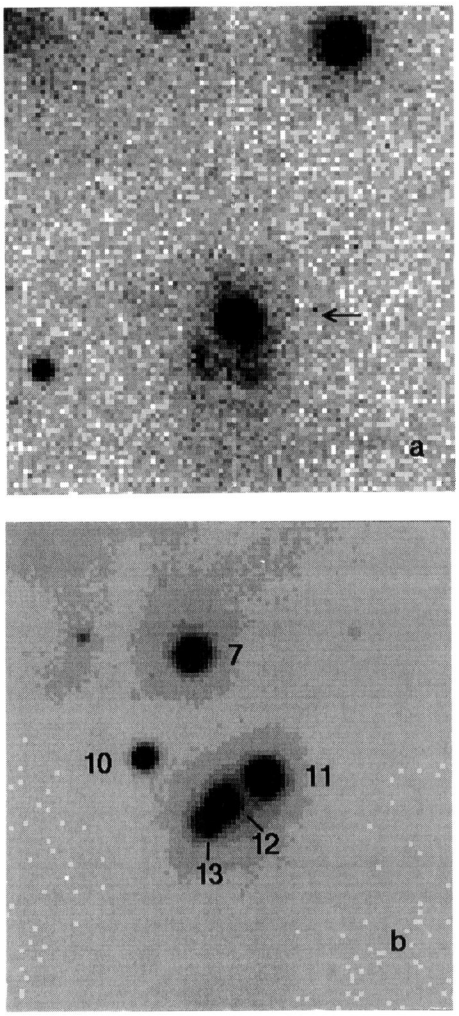

Fig. 4. a and b. Enlargements of the R frame showing S 187Hα and its associated reflection nebula **a**, and of the V frame showing the exciting cluster at the center of S 187B **b**

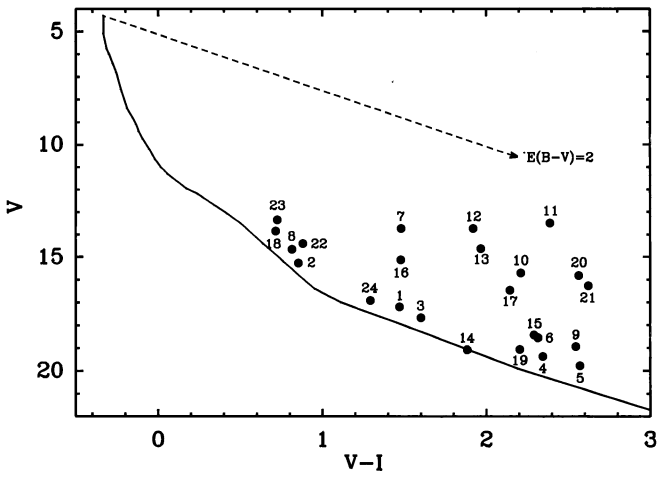

Fig. 5. V versus $V-I$ diagram. The main-sequence (from Bessell 1979, for a distance modulus of 10) is indicated along with the reddening line for an O5V star with 6.2 mag of visual extinction

concerns relative intensity measurements inside a given spectral range. Of course, the accuracy of the absolute fluxes is not as good, as it depends on the photometric quality of the night, on the position of the object in the slit, and on the seeing ($\gtrsim 2''$). Basic wavelength calibration was achieved using neon and argon calibration arcs; small corrections were later applied based on several telluric OH emission lines, whose wavelengths are derived from Coxon et al. 1981 and Coxon (private communication; cf. also Osterbrock & Martel 1992). This correction (< 15 km s^{-1}) is probably due to differences in pupil illumination between the arcs and the sky.

4.2. Results

Figure 6 shows two spectra of S 187Hα, one in each spectral range. The strongest lines are identified. These spectra are characteristic of pre-main-sequence stars. They present similarities with spectra of well known YSOs like V645 Cygni (Hamann & Persson 1989), GL 490 (Persson et al. 1988), and AS 353A (Eislöffel et al. 1990); see also the numerous spectra, in the near infrared, of T Tauri stars by Hamann & Persson 1992a (hereafter HP1) and of Herbig Ae/Be stars by Hamann & Persson 1992b (hereafter HP2). In the Hα range, the spectrum of S 187Hα exhibits a very broad Hα line with a double peak. The [N II] lines at 6548.05 Å and 6583.46 Å, and the [S II] lines at 6716.41 Å and 6730.79 Å, which are visible in the spectrum of the H II region S 187B, are not seen in the spectrum of S 187Hα. Several lines of Fe I and Fe II are present. The spectrum in the near infrared range is strongly dominated by the Ca II triplet at 8498 Å, 8542 Å, and 8662 Å. These lines have nearly equal intensity. The O I line at 8446.5 Å is relatively strong. Numerous lines of Fe I are also present. The Paschen recombination lines are weak. A few lines have not been identified.

The measurements are summarized in Table 3. Column 1 gives the wavelengths and column 2 the line identifications. The wavelengths of identified lines are from Moore (1959). Column 3 gives the observed fluxes, not corrected for interstellar reddening, and column 4 the equivalent widths of the lines. The fluxes were obtained from the 1992 January spectra, which we consider the most reliable; the equivalent widths were measured on a composite of four spectra.

The LSR velocities and the FWHMs (corrected for the instrumental broadening) of the strongest lines were determined from each spectrum. In columns 3 and 4 of Table 4 we give the mean values and the standard errors of these measurements. Kinematical data for the H II region, for the associated molecular cloud, and for the H_2O maser are given for comparison.

4.3. S 187Hα

4.3.1. The hydrogen recombination lines

Hα is the brightest and the broadest line in the observed spectrum of S 187Hα. Its equivalent width of 123 Å is comparable to that of the most extreme Herbig Ae/Be or T Tauri stars (Cohen & Kuhi 1976, Levreault 1988, HP1, HP2). Its Hα lu-

Table 3. Identifications and fluxes of the observed lines. Dominant lines of blends are indicated by *

λ_0 (Å)		Identification	Flux (10^{-17} erg s^{-1} cm^{-2})	W_λ (Å)
6327–6328		?	181:	0.5:
6335.335		Fe I (62)	805	1.56
6336.835		Fe I (816)		
6344.154		Fe I (169)	204:	0.4:
6358.692		Fe I (13)	1092	2.33
6360	*	?		
6362.889		Fe I (1019)?		
6369.450		Fe II (40)	363	0.8
6393.635		Fe I (168)	613	1.28
6400.010		Fe I (816)	410	0.73
6407.300		Fe II (74)?	127:	0.3:
6408.031		Fe I (816)		
6411.658		Fe I (816)	230:	0.5:
6416.905		Fe II (74)?	848	1.76
6421.355		Fe I (111)	307:	0.9:
6430.851		Fe I (62)	1462	2.72
6432.654	*	Fe II (40)		
6439.075		Ca I (18)?	256:	0.55:
6449.808		Ca I (19)?	64:	0.2:
6456.376		Fe II (74)	939	1.70
6462.731		Fe I (168)	212:	0.4:
6481.878		Fe II (199)?	451:	0.7:
6493.050		Fe II?	1382	2.18
6494.985	*	Fe I (168)		
6498.950		Fe I (13)?		
6508.135		Fe II?	123:	0.2:
6515.703		Fe II?	2260	3.62
6516.053	*	Fe II (40)		
6518.376		Fe I (342)?		
6546.245		Fe I (268)	314:	
6562.800		Hα	71149	123.32
6592.919	*	Fe I (268)	916	1.33
6593.878		Fe I (168)		
6606–6607		?	628	1.23
6609.116		Fe I (206)		
6643–6644		?	374:	0.6:
6663.446		Fe I (111)	345	0.39
6677.993		Fe I (268)	949	1.17
6678.100		He I (46)?		
6725.39		Fe I (1052)?	425	0.80
6726.668		Fe I (1197)?		
8382.54		Ti I (33)?	234:	0.2:
8382.82		Ti I (33)?		
8387.781	*	Fe I (60)	4220	4.28
8392.400		P20		
8399–8400		?	148:	0.2:
8412.36		Ti I (33)?	469	0.52
8413.321		P19		
8426.50		Ti I (33)?	86:	0.1:
8434.98		Ti I (33)?	1001	1.10
8435.68		Ti I (33)?		
8437.958		P18		
8439.603		Fe I (1172)		
8446.50		O I (4)	6252	6.78

Table 3. (continued)

λ_0 (Å)		Identification	Flux (10^{-17} erg s^{-1} cm^{-2})	W_λ (Å)
8451.010		Fe II?	345:	0.4:
8467.256		P17	1959	2.12
8468.413	*	Fe I (60)		
8486		?	354	0.38
8498.018	*	Ca II (2)	38956	40.15
8502.487		P16		
8514.075	*	Fe I (60)	2496	2.64
8515.08		Fe I (401)		
8542.049	*	Ca II (2)	45874	47.40
8545.384		P15		
8582.267		Fe I (401)	390	0.42
8594		?	1300	1.37
8598.394	*	P14		
8611.807		Fe I (339)	1639	1.72
8621.612		Fe I (401)	209	0.22
8661.908		Fe I (60)	41769	43.8
8662.140	*	Ca II (2)		
8665.021		P13		
8674.751	*	Fe I (331)	1443	1.51
8675.38		Ti I (68)?		
8682.990		Ti I (68)?	89:	0.1:
8688.633		Fe I (60)	2227	2.29
8727–8728		?	291:	0.3:
8729.12		Fe I (713)?		
8734.70		Ti I (68)?	215:	0.2:
8747.320		Fe I (401)	2161	2.20
8750.475	*	P12		
8757.192		Fe I (339)	670	0.68

minosity, corrected for a visual extinction between 4 and 7 mag (see the justification in Sect. 5), is in the range 0.5 $L_\odot$ to 5 $L_\odot$. S 187Hα is comparable to the brightest of the pre-main-sequence stars studied by Levreault (1988), of which only three have an Hα luminosity greater than 1 $L_\odot$: AFGL 490 with $L_{H\alpha} = 3.7\ L_\odot$, V645 Cyg with $L_{H\alpha} = 21\ L_\odot$ and MWC 1080 with $L_{H\alpha} = 109\ L_\odot$.

We have measured an Hα/Hβ Balmer decrement of 18 on a low resolution spectrum taken for us by E. Bertin. Assuming the standard extinction law (Mathis & Savage 1979) and optically thin case B emission at 10^4 K by a photoionized plasma (as in classical H II regions; Brocklehurst 1971), we estimate the following color excess and extinction (Caplan & Deharveng 1986) of S 187Hα: $E_{\beta-\alpha} = A_{H\beta} - A_{H\alpha} = 2$ mag, A_V(Balmer)= 5.2 mag; this figure is smaller than the extinction of 6.8 mag found for the exciting stars of the associated H II region. From the observed Hα flux, with the same assumptions, we expect a radio continuum flux density for S 187Hα at 1.4 GHz of about 40 mJy. Such a source should have been detected by Snell & Bally (1986). This is clearly not the case, which indicates that S 187Hα is not a compact H II region.

The alternative is that the observed emission in S 187Hα (both hydrogen recombination lines and radio continuum) comes from an ionized wind (Panagia & Felli 1975, Panagia 1991 and references therein). For a fully ionized and spherical

wind, with a terminal velocity of about 500 km s^{-1} (inferred from the Hα profile – see below), with a mass loss of 10^{-6} $M_{\odot}$ $year^{-1}$ or less (as obtained for a few Herbig Ae/Be stars by Skinner et al. 1993), the expected radio continuum flux density at 1.4 Ghz would be smaller than 0.1 mJy, i.e. below the sensitivity limit reached by Snell and Bally (1986).

The Paschen recombination lines are present in the near infrared spectra. These lines are weak and often blended with others (cf. Table 3 and Fig. 6); however, the fluxes of the P12 and P14 lines are reliable, and allow another estimation of the extinction, discussed in Sect. 5.

The Hα line profile is presented in Figure 7 along with the Ca II 8542 Å profile. Hα is very broad, more than 1000 km s^{-1} from wing to wing. It has a double-peaked shape. The primary emission peak is at -24 km s^{-1}, consistent with the velocity of the associated molecular cloud. The line is asymmetric, with a blueshifted absorption feature at -181 km s^{-1} and an additional weak emission peak even further blueward, at -289 km s^{-1}. This is a Beals Type III P Cygni profile (Beals 1951). This Hα profile is common in classical T Tauri stars (Basri 1990), and much effort has gone into its interpretation. Spherically symmetric and homogeneous wind models (Hartmann et al. 1990) tend to produce Hα line profiles with much deeper absorption reversals than observed here; furthermore, the models' main emission peak is too redshifted and the intensity decrease on the blue side is not steep enough to match the observations. Non-spherical – conical – wind models have been developed by Calvet et al. (1992) to account for winds originating in a boundary layer between the rotating star and the circumstellar disk. Both these turbulent and rotating wind models have difficulty reproducing Beals's Type III P Cygni profiles, especially the centrally peaked emission. Quite different models, of infalling envelopes with conical geometry, intended to simulate accretion from a circumstellar disk (Calvet & Hartmann 1992), also fail to reproduce the observed Hα profile; the blue peak is too strong, and the red peak is too redshifted. Only the stochastic wind model developed by Mitskevich et al. (1993) successfully reproduces observed Beals Type III profiles. In this model, the

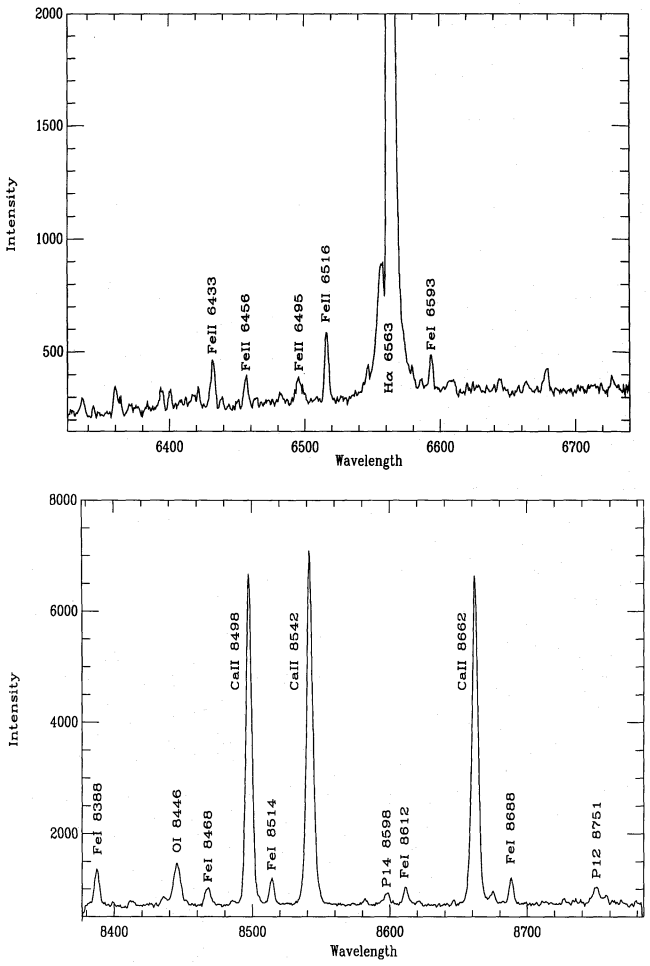

Fig. 6. Spectra of S 187Hα in the Hα range (top) and the near infrared range (bottom). Each spectrum shown is a composite of the four observed spectra. The principal lines are identified

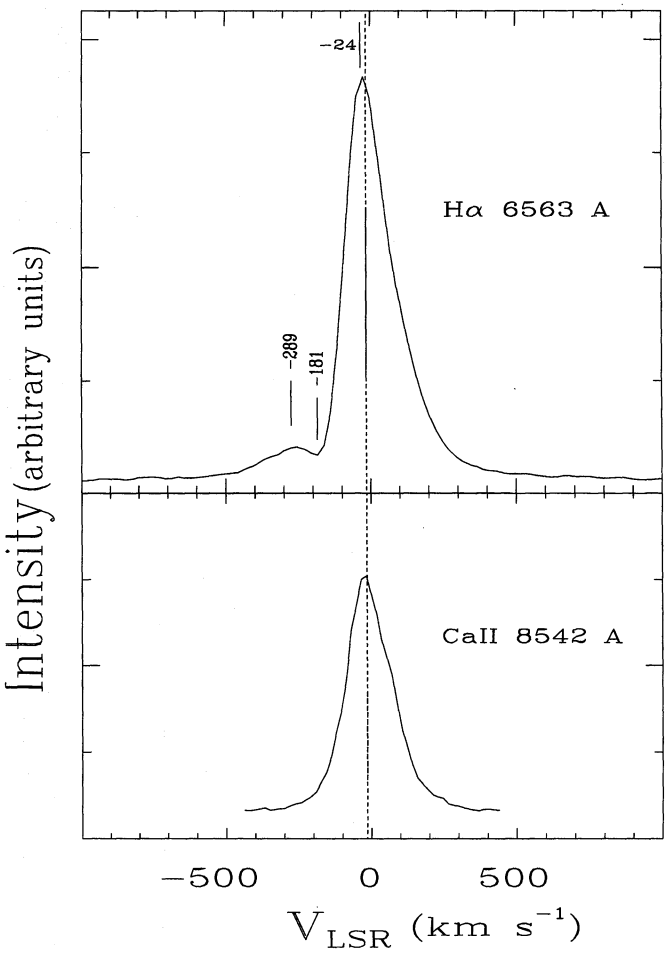

Fig. 7. Hα and Ca II (8542 Å) LSR velocity profiles for S 187Hα (not corrected for instrumental broadening). The dashed line at -15 km s^{-1} corresponds to the molecular cloud's mean velocity. The velocity positions for the Hα line correspond to the mean values given in Table 4

Table 4. Kinematical observations

λ_0 (Å)	Ident.	V_{LSR} (km s^{-1})	FWHM (km s^{-1})	Ref.
		S 187Hα		
6562.80	Hα (primary)	−24. ± 8.	164. ± 3.	
6562.80	Hα (secondary)	−289. ± 18.		
6562.80	Hα (absorp.)	−181. ± 14.		
6516.05	Fe II (40)	−10. ± 15.	117. ± 18.	
8446.50	O I (4)	−49. ± 13.	185. ± 4.	
8387.78	Fe I (60)	−11. ± 5.	116. ± 16.	
8514.08	Fe I (60)	−6. ± 3.	119. ± 20.	
8688.63	Fe I (60)	−19. ± 5.	114. ± 16.	
8498.02	Ca II (2)	−19. ± 3.	150. ± 5.	
8542.05	Ca II (2)	−15. ± 2.	164. ± 8.	
8662.14	Ca II (2)	−19. ± 3.	158. ± 6.	
		The H II region		
	H109α	−14.6		a
6562.80	Hα	−7.6 ± 0.3	34.6 ± 0.6	b
6562.80	Hα	−5. ± 2.		
6548.05	[N II]	−11.9 ± 1.7		
6583.46	[N II]	−7.7 ± 0.9	30. ± 15.	
6716.41	[S II]	−4. ± 6.	(mean width	
6730.79	[S II]	−3. ± 10.	of all 5 lines)	
		The molecular cloud		
	^{13}CO	−14.9 ± 0.4	3.5	c
	^{12}CO	−14.0		d
	NH_3	−13.51 ± 0.02	0.94 ± 0.05	e
	HCN	−15.9 ± 0.2	4.7 ± 0.4	f
		The H_2O maser		
	H_2O	−15 to −13		g

a Rossano (1978)
b Fich et al. (1990)
c Blitz et al. (1982)
d Casoli et al. (1984a)
e Torrelles et al. (1986)
f Burov et al. (1988)
g Henkel et al. (1986)

wind is clumpy and decelerates at large distances from the star. The Hα line has a very large optical thickness. Some of their case A models (clump sizes of the order of 0.1–0.3 stellar radii, filling factors in the 0.1–0.3 range) account very well for most of the observed features: a double-peaked profile with the blue peak much smaller than the red one; a red peak velocity near zero with a blue peak blueshifted; a very sharp transition between the absorption and the red emission.

The Hα emission profile of S 187Hα is very similar to that of V645 Cyg, knot N0 (cf. Fig. 7 in Goodrich 1986). A circumstellar disk plus bipolar wind model has been proposed to account for the observed spectrum of V645 Cyg (Hamann & Persson 1989). Knots N0 and N1, the optical counterparts of the YSO V645 Cyg, sample two different lines of sight to the central object and exhibit different Hα profiles. N1 has a true P Cygni profile whereas N0 exhibits a Beals Type III profile. Here again, the clumpy wind model of Mitskevich et al. (1993), although spherical, can successfully explain how two different lines of sight can exhibit two different Hα profiles.

4.3.2. The Ca II triplet lines

The near infrared spectrum of S 187Hα is dominated by the Ca II triplet emission lines at 8498 Å, 8542 Å, and 8662 Å.

S 187Hα has very large Ca II equivalent widths, of the order of 40 Å or more. When we compare with those of T Tauri stars (HP1), of Herbig Ae/Be stars (HP2), and with those of a few massive YSOs (McGregor et al. 1984, Persson et al. 1988, Hamann & Persson 1989), we find that only a few objects have higher equivalent widths.

The luminosity of the Ca II 8542 Å line, corrected for the contribution of the Paschen 15 line and for a visual extinction 4 mag $\leq A_V \leq$ 7 mag, is in the range 0.10 $L_\odot$ to 0.44 $L_\odot$. This luminosity is very high; it is more typical of Herbig Ae/Be stars than of T Tauri stars (cf. the diagram of the Ca II 8542 Å luminosity versus spectral type in HP2, Fig. 5), and is comparable to that of objects like V645 Cyg, MWC 137, and V380 Ori.

As discussed by Herbig & Soderblom (1980), the Ca II triplet emission lines are optical thick. For optically thin emission the 8498 Å, 8542 Å, and 8662 Å line intensities are in the ratios 1:9:5, respectively, whereas in S 187Hα the observed fluxes are in the ratios 1:1.17:1.05. Although optically thick, the Ca II triplet lines are nearly gaussian. They are centrally peaked, with a mean velocity which is nearly that of the associated molecular cloud (Table 4). They are broad, with FWHMs of 150 km s^{-1}, 164 km s^{-1}, and 158 km s^{-1} respectively for the 8498 Å, 8542 Å, and 8662 Å lines. Grinin & Mitskevich (1988, 1990) have shown that an intermediate optical depth (of 3 to 10) is sufficient to account for the near equality of the Ca II triplet intensities. This being explained, the stochastic wind model of Mitskevich et al. (1993) is able to reproduce the broad, nearly symmetric, centrally peaked Ca II triplet lines.

4.3.3. The O I 8446 Å line

With an equivalent width of 6.8 Å and a luminosity, after correction for a visual extinction between 4 mag and 7 mag, in the range 0.015 $L_\odot$ to 0.065 $L_\odot$, the O I 8446 Å emission in S 187Hα is relatively strong, as is generally the case in YSOs. This transition originates from a level situated some 11 eV above the ground state; such a high energy level cannot be collisionally excited in S 187Hα (see Sect. 4.3.4). Bowen (1947) suggested that the presence of O I 8446 Å emission in cool stars could be due to Lyβ fluorescence. The $3d\,^3D^0$ level of neutral oxygen, at about 12 eV, is excited by Lyβ fluorescence. A permitted transition allows population of the lower $3p\,^3P$ level

from which the O I 8446 Å line originates. This explanation is now commonly accepted to account for the strong O I 8446 Å emission observed in YSOs (cf. Felenbok et al. 1988 for a discussion of the O I emission in Herbig Ae stars and Hamann & Simon 1988 for a discussion of the O I emission in the peculiar YSO MWC 349A). In S 187Hα, the O I/Hα ratio corrected for an extinction 4 mag $\leq A_V \leq$ 7 mag, lies in the range 0.01 to 0.03. Morgan (1971) showed that if both O I and Hα emission is due to reabsorption of Lyβ, then the O I/Hα ratio should be less than 4 10^{-5} for optically thin emission. The much larger value obtained for S 187Hα indicates that the region emitting the O I line has a very large optical thickness in Hα. Many Lyβ photons are produced and they are recycled many times, so that many are eventually absorbed by an oxygen atom in the ground state. As explained by McGregor et al. (1984), the Lyβ fluorescence mechanism requires not only the presence of Lyβ photons, but

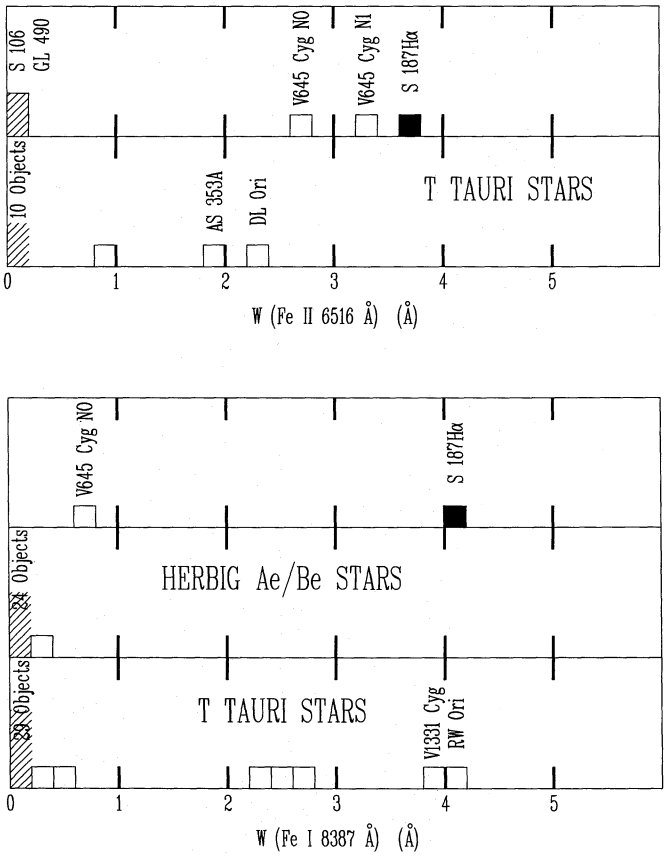

Fig. 8. Equivalent widths of the Fe I 8387.8 Å and the Fe II 6516.1 Å lines for various pre-main-sequence objects

also that oxygen be mostly neutral and (because of the efficient charge-exchange reactions between O^0 and H^+) that hydrogen also be mostly neutral in the O^0 emitting region. Thus O I emission probably occurs in a dense H I–H II transition region, where hydrogen is only partially ionized.

The line at 8446 Å is a blend of three transitions of the same multiplet. These transitions lie within 0.5 Å (18 km s^{-1}) of each other, so that the profile of the line is only slightly affected. In S 187Hα the O I line is symmetric, with a measured FWHM of about 185 km s^{-1}.

4.3.4. The Fe I and Fe II lines

Emission from several multiplets of Fe I and Fe II are present in the spectra. Their equivalent widths are large compared to those of other pre-main-sequence objects (Fig. 8), whatever the line or the ionization state (Fe^0 or Fe^+).

The strongest Fe I lines observed are, in the near infrared range, those of the Fe I (60) multiplet, at 8387.8 Å, 8468.4 Å, 8514.1 Å, and 8688.6 Å, which come from a level situated 3.7 eV above the ground state. Several other Fe I lines are observed, especially those of the Fe I (816) multiplet, whose upper level is situated some 5.6 eV above the ground state. No line originating from a higher energy level is observed.

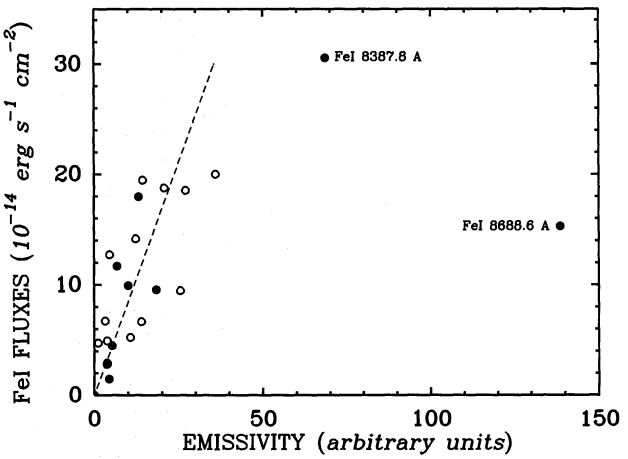

Fig. 9. Fe I line fluxes, corrected for a visual extinction of 4 mag, versus ε' for a temperature of 5000 K. The filled circles refer to lines in the near infrared range, open circles to lines in the Hα range

The emissivity of an Fe I line, assuming local thermodynamic equilibrium, is proportional to $\varepsilon' = gf\lambda^{-3}e^{-E/kT}$, where T is the temperature of the emitting region. The gf and E values can be found in Kurucz (1981). Figure 9 shows the Fe I fluxes, corrected for an extinction $A_V = 4$ mag (see below), as a function of ε' for $T = 5000$ K. For optically thin emission, the fluxes are proportional to the emissivities, hence to the ε' values. Indeed, for the Fe I lines in the near infrared range, a proportionality between fluxes and emissivities is observed; only the strong Fe I line at 8688.6 Å (and possibly the line at 8387.8 Å) lies under the regression line, and thus appears to be optically thick. Due to the large extinction, the fluxes of the Fe I lines in the Hα range are less accurately determined; this explains the larger dispersion of the points around the regression line. However, here again, a proportionality relation is found between flux and emissivity; all the Fe I lines in the Hα range appear to be optically thin. The constant of proportionality between fluxes

and emissivities must be the same for the Fe I lines in the Hα and near infrared ranges. This allows an independent determination of the extinction, A_V, of about 4 mag. If A_V is greater than 4 mag, the extinction-corrected fluxes of the Fe I lines in the Hα range are too high with respect to those in the near infrared. Of course, this estimate of the extinction depends on the temperature assumed for the plasma; one gets a higher A_V – about 6 mag – if one assumes the higher but still plausible temperature of 8000 K (in which case Fe I at 6400 Å is also optically thick). We shall return to this point in Sect. 5.

The Fe I (60) lines are centrally peaked, nearly gaussian, with a FWHM of the order of 115 km s^{-1}, much smaller than those of the Ca II, O I and Hα lines.

In the Hα range, the strongest Fe II lines are those of the Fe II (40) and Fe II (74) multiplets. These lines originate from levels situated respectively at 4.8 eV and 5.8 eV above the ground state, a situation comparable to that of the Fe I lines. However, the gf values of the Fe II transitions are so small that these lines would not be observable if the excitation mechanism were the same as for Fe I. So how are these energy levels populated? Persson et al. (1988) (see also Johansson & Jordan 1984) suggest that some Fe^+ levels at about 11 eV may be populated by Lyα fluorescence from the a^4D state. The detailed study of MWC 349A by Hamann & Simon (1988) shows that this Lyα pump is active there. However, Hamann & Simon present evidence from line profile analysis showing that the intermediate energy levels (including the upper levels of the Fe II (40) and Fe II (74) multiplets) are probably not populated by radiative cascades from the upper pumped levels. The problem remains unsolved.

The Fe II (40) line at 6516.05 Å is symmetric and nearly gaussian, with a mean velocity (-10 ± 15 km s^{-1}) close to that of the associated molecular cloud. This Fe II 6516 Å line is not very broad, with a FWHM of 117 ± 18 km s^{-1}. Thus this Fe II line is very similar in shape to all the Fe I lines, and differs from the much broader Ca II, O I, and Hα lines. The discrepancy between the Fe II 6516 Å and the O I 8446 Å line profiles is particularly interesting, as it shows that these two lines are not emitted in the same volume.

A weak line observed near 8450 Å has been tentatively identified as Fe II at 8451.02 Å (transition e^6D–$5p^6F$) which originates from one of the high energy levels excited directly by Lyα fluorescence (see Fig. 4 in Hamann & Simon 1988).

4.3.5. Uncertain identifications and non-identified lines

A number of weak lines in Table 3 have been tentatively attributed to Ti I. Their fluxes, compared to those of Fe I, are consistent with LTE and cosmic abundances. Four lines seem to belong to the Ti I (33) multiplet (8382.54 Å, 8412.36 Å, 8426.50 Å, and 8434.98 Å), and three others (8675.38 Å, 8682.99 Å, and 8734.70 Å) apparently belong to the Ti I (68) multiplet; these correspondences add weight to the identification. The lines at 6439.1 Å and 6449.9 Å are possibly Ca I, corresponding to the strongest lines of the Ca I (18) and Ca I (19) multiplets.

A few lines are not identified. The strongest of these are at 6360 Å, 6643 Å, and 8486 Å.

5. Discussion

5.1. The extinction of S 187Hα

The extinction of S 187Hα is difficult to estimate. An A_V of 5.2 mag is derived from the observed Balmer decrement (Sect. 4.3.1), assuming optically thin case B emission by a photoionized plasma with at 10^4 K and an electron density of 10^4 cm^{-3} (Brocklehurst 1971). However, the hydrogen recombination lines, especially the bright Hα, are probably optically thick, in which case the extinction is underestimated. Also, the hydrogen recombination lines are not emitted in a compact H II region but in an ionized stellar wind, and the theoretical Balmer decrement is unknown. The Hβ and Paschen lines are probably less optically thick; they also span a larger spectral range, thus allowing a better determination of the extinction. With the same assumptions we derive $A_V \approx 6.2$ mag from the observed Hβ/P12 and Hβ/P14 ratios.

The extinction can be derived from a comparison of the Fe I line intensities in the Hα range and in the near infrared range (Sect. 4.3.4); however, this estimate depends on the temperature of the plasma, which is unknown. We find $A_V \approx 4$ mag for $T =$ 5000 K and $A_V \approx 6$ mag for $T = 8000$ K. This latter temperature is high, but plausible; in their models, Grinin & Mitskevich (1988, 1990) consider stellar winds in the 7000–8000 K range.

An A_V of 6.1 mag is derived from the observed V and $B-V$ using the method described by Hillenbrand et al. (1992). This procedure assumes that S 187Hα lies close to the main sequence in the V versus $B-V$ diagram. However, as discussed by Hamann & Persson (1992c), some of the visual light may be reflected by dust; this would lead to measured colors bluer than the intrinsic ones, and thus to an underestimate of the extinction. Further underestimation may be caused by the veiling spectrum.

Although each of the procedures used to derive the extinction can be criticized, the figures obtained from the different methods are rather close. The extinction of S 187Hα is probably in the 4–7 mag range; we favor a value for A_V of 6 mag.

5.2. The spectral energy distribution of S 187Hα

Figure 10 presents the spectral energy distribution of S 187Hα corrected for a visual extinction of 6.1 mag. The corrections were made assuming an extinction law typical of the interstellar medium (Mathis 1990, with $R = 3.1$). For comparison we present the energy distribution of a B8 V star, whose emission matches the visible continuum emission of S 187Hα. S 187Hα clearly shows an excess of near infrared emission; this conclusion stands for any value of A_V in the range 4–7 mag. The spectral energy distribution of S 187Hα is very similar, both in shape and intensity (allowing for the distance), to that of R Mon (Hillenbrand et al. 1992, Hamann & Persson 1992c). Like R Mon, S 187Hα has a spectrum which rises in the infrared and presents an inflection in its spectral distribution be-

tween 1 μm and 2 μm. S 187Hα may belong to the Group II of Hillenbrand et al. (1992); these objects are interpreted as star-disk systems still surrounded by gas and dust; the inner regions of the accretion disk must be optically thin (free of warm dust) to account for the inflection in the spectral energy distribution. Hamann & Persson (1992c) emphasize the part played by reflected light. S 187Hα may belong to their group of reflection sources, which contains V645 Cyg and R Mon; in these objects a certain fraction of the observed visual light is probably light reflected by dust.

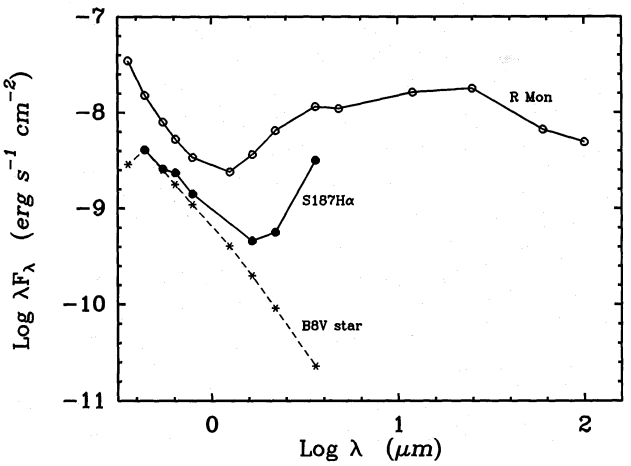

Fig. 10. Extinction-corrected spectral energy distributions. Solid circles are for S 187Hα assuming $A_V = 6.1$ mag. Open circles are for R Mon, according to Hillenbrand et al. 1992. The dashed line corresponds to the energy distribution of a B8 V star, which matches the visible continuum emission of S 187Hα.

6. Conclusions

We have discovered a strong Hα-emitting stellar object at the edge of the S 187 H II region. This object is a pre-main-sequence star. The evidence is: it is situated in a region of active star formation (where a compact infrared source, a CO outflow, and an H_2O maser have already been found); it is highly reddened, with a visual extinction in the 4–7 mag range; it is associated with a small conical reflection nebula; and its spectrum displays very bright and broad emission lines, typical of pre-main-sequence objects. The spectrum of S 187Hα is very similar to those of well known YSOs such as R Mon, V645 Cyg, and MWC 1080.

It is difficult to determine whether this object is a T Tauri or a Herbig Ae/Be star. Our low resolution observations, from 4400 Å to 8800 Å, show no photospheric absorption lines, so its spectral type cannot be estimated. Higher spectral resolution in the 4000 Å – 6000 Å range are needed to address this question. Among the numerous spectra of YSOs presented by Cohen & Kuhi (1979), the most similar is that of R Mon, which has been classified by these authors as a B0, and which has a bolometric luminosity of 1000 $L_\odot$ (Levreault 1988). A direct estimate of the luminosity of S 187Hα is, at the moment, difficult because this object is observed in the direction of the H II region S 187, which is an extended IRAS source, so that confusion impedes measurement of the infrared emission of S 187Hα. Only indirect evidence is left. For example, its B and V magnitudes correspond to a late B star with a near infrared excess. Also, the luminosity in the Hα and Ca II triplet emission lines is more typical of Herbig Be to early Ae stars than of T Tauri stars. However, HP2 have shown that Herbig Be stars are relatively more effective emitters of the Paschen 12, O I 8446 Å, and Fe II lines than of Ca II 8542 Å; this suggests that hotter stars have hotter or more ionized emitting regions. For this reason, S 187Hα is probably not an early Herbig Be star; the Ca II lines are too strong with respect to the nearby Paschen lines or even with respect to the O I 8446 Å line (the P12/Ca II ratio of 0.05 and the O I/Ca II ratio of 0.14 indicate that S 187Hα is probably no hotter than a Herbig Ae type star; cf. Fig. 7 in HP2). Our conclusion is that S 187Hα is most probably a Herbig late Be star or early Ae star.

S 187Hα presents many characteristics of the "outflow group" of Herbig Ae/Be stars, identified by HP2, and which contains V645 Cyg, R Mon, and V380. *i*) The Hα line is very broad, with a maximum velocity exceeding 500 km s^{-1}, and has an almost P Cygni profile. *ii*) The O I, Ca II triplet and Fe lines are symmetric and single-peaked. *iii*) The weakest lines (and probably the least optically thick) are the narrowest; Hα is the broadest line of the spectrum, the Ca II lines are narrower, and the weak iron lines are narrower still. *iv*) The emission of neutral species is observed (Fe^0, Ti^0, and possibly Ca^0); also, Ca II emission is strong with respect to O I and Paschen 12. As stressed by HP2, this subgroup of "outflow" Herbig Ae/Be stars displays many similarities with the classical T Tauri stars. These similarities suggest that the models of classical T Tauri stars may also apply to these Herbig stars: most of the line emission would arise from a dense, turbulent region located near the star/accretion–disk boundary layer.

The spectral energy distribution of S 187Hα in the 4500 Å – 3.6 μm range is similar in shape to that of R Mon and V645 Cyg; these distributions are well explained by star-disk systems, depleted of dust close to the star, and still surrounded by gas and dust.

In conclusion, S 187Hα appears to be a young stellar object very similar, both in luminosity and geometry, to V645 Cyg – which has been classified as O7 by Cohen (1977) and as A0–A5 by Goodrich (1986) – and to R Mon – spectral type B0 according to Cohen & Kuhi (1979).

Acknowledgements. We wish to acknowledge the contributions of C. Henkel, J.A. Coxon, J. Bally, F. Casoli, and G. Joncas to many aspects of this study. We are indebted to F. Sèvre for his efforts in obtaining good H, K, and L magnitudes of S 187Hα, and to E. Bertin for providing us with a low resolution spectrum of this object. We thank C. Catala and J.P. Baluteau for helpful discussion and comments on this manuscript. J. Lombard has been most helpful with the data reduction.

Appendix

The coordinates were determined by using those stars in our field which are also in the Guide Star Catalog (GSC). We decided to work in the B1950 system, since all the existing optical, infrared, millimeter, and radio results on the S 187 region are in B1950 coordinates. Therefore we converted the GSC's coordinates – for equinox J2000 and for epoch J1987.06 – to coordinates for equinox B1950 and for the epoch of our observations, which is B1990.72. (The coordinates are different for different *equinoxes* – different coordinate frames – because of precession and also because of the shift between the F4 and F5 systems; the *epoch* – the moment of the observation – comes into play because of the stars' proper motions.) The first step, at least in principal, was to convert the GSC positions to equinox *and* epoch J2000 coordinates, by applying the proper motions over the intervening 12.94 years. We assumed these proper motions to be zero. Next, using the procedure outlined in the Explanatory Supplement to the Astronomical Almanac (Seidelmann 1992) we converted from J2000 (equinox *and* epoch) to B1950 (equinox *and* epoch). Finally we applied the B1950 proper motions provided by this conversion (they are *not quite* the same as the J2000 values) to arrive at the epoch B1990.72 coordinates. Of course the true proper motions are unknown, but in fact the result is practically independent of the values that are assumed, as long as the beginning and end epochs are about the same. On the other hand, *ignoring* the proper motions and converting from epoch J2000 to epoch B1950 gives a result differing by about $0\farcs2$.

Five GSC stars are found in our frames. Three of these – GSC4030–1313 (our No. 7 in Table 1), GSC4030-1388 (our No. 23), and GSC4034–0951 (an object not in Table 1) – are designated as "stellar", and are usable as positional references. The other two – GSC4030–1292 (our No. 11) and GSC4030–1835 – are designated as "non-stellar". The former is in fact a single star with some nearby nebulosity, but usable as a reference; the latter is unusable because it is in fact two stars $4''$ apart (our Nos. 12 and 13).

The positions of these reference stars were projected onto the plane tangent to the field center to give their "standard" coordinates X, Y. Then, by least squares, we determined the four parameters A, B, C, and D which map the observed x, y to X, Y using the simplest possible model (cf. Deharveng et al. 1992):

$$x = AX - BY + C, \text{ and}$$
$$y = BX + AY + D.$$

The standard error (quadratically combined error in both coordinates) is $0\farcs45$.

We then used these parameters to calculate the right ascensions and declinations of all the stars in the field. For consistency, the coordinates of *all* the stars in Table 1, including the reference stars, were calculated in this way. The relative positional uncertainty in Table 1 is therefore of the order of $0\farcs5$, whereas the absolute uncertainty is essentially that of the GSC, or about $1''$.

References

Bally J., Lada C.J., 1983, ApJ 265, 824
Basri G., 1990, Mem.Soc.Astron.Ital. 61, 707
Beals C.S., 1951, Publ. Dominion Astrophys. Obs. 9, 1
Bessell M.S., 1979, PASP 91, 589
Blitz L., Fich M., Stark A.A., 1982, ApJS 49, 183
Burov A.B, Kislyakov A.G., Krasil'nikov A.A., Kukina E.P., Lapinov A.V., Pirogov L.E., Vdovin V.F., Zinchenko I.I., 1988, Sov.Astron.Lett. 14, 209
Bowen I.S., 1947, PASP 59, 196
Brocklehurst M., 1971, MNRAS 153, 471
Calvet N., Hartmann L., 1992, ApJ 386, 239
Calvet N., Hartmann L., Hewett, R., 1992, ApJ 386, 229
Caplan J., Deharveng L., 1986, A&A 155, 297
Casoli F., 1986, Protostars and molecular clouds, T. Montmerle and C. Bertout (eds.), p. 36
Casoli F., Combes F., Guérin M., 1984a, A&A 133, 99
Casoli F., Combes F., Guérin M., 1984b, Nearby molecular clouds, G. Serra (ed.), Lecture Notes in Physics no. 237, p. 136 Springer-Verlag, Berlin-Heidelberg
Chevalier C., Ilovaisky S.A., 1991, A&AS 90, 225
Christian C.A., Adams M., Barnes J.V., Butcher H., Hayes D.S., Mould J.R., Siegel M., 1985, PASP 97, 363
Cohen M., 1977, ApJ 215, 533
Cohen M., Kuhi L.V., 1976, ApJ 210, 365
Cohen M., Kuhi L.V., 1979, ApJS 41, 743
Cousins A.W.J., 1976, MNRAS 81, 25
Coxon J.A., Foster S.C., 1981, Can.J.Phys. 60, 1982
Deharveng L., Caplan J., Lombard J., 1992, A&AS 94, 359
Eislöffel J., Solf J., Böhm K.H., 1990, A&A 237, 369
Felenbok P., Czarny J., Catala C., Praderie F., 1988 A&A 201, 247
Fich M., Blitz L., 1984, ApJ 279, 125
Fich M., Treffers R.R., Dahl G.P., 1990, AJ 99, 622
Finkenzeller U., Mundt R., 1984, A&AS 55, 109
Georgelin Y.M., 1975, Thesis, Université de Provence, Marseille
Goodrich R.W., 1986, ApJ 311, 882
Grinin V.P., Mitskevich A.S., 1988, Izv.Krymsk.Astrofiz.Obs. 78, 28
Grinin V.P., Mitskevich A.S., 1990, Astrofizika 32, 383
Hamann F., Persson S.E., 1989, ApJ 339, 1078
Hamann F., Persson S.E., 1992a, ApJS, 82, 247 (HP1)
Hamann F., Persson S.E., 1992b, ApJS, 82, 285 (HP2)
Hamann F., Persson S.E., 1992c, ApJ 394, 628
Hamann F., Simon M., 1988, ApJ 327, 876
Hartmann L., Calvet N., Avrett E.H., Loeser R., 1990, ApJ 349, 168
Henkel C., Haschick A.D., Güsten R., 1986, A&A 165, 197
Henning T., 1990, Fundamentals of Cosmic Physics 14, 321
Herbig G.H., Soderblom D.R., 1980, ApJ 242, 628
Hillenbrand L.A., Strom S.E., Vrba F.J., Keene J., 1992, ApJ 397, 613
Israel F.P., 1977 A&A 61, 377
Johansson S., Jordan, C., 1984, MNRAS 210, 239
Joncas G., Durand D., Roger R.S., 1992, ApJ 387, 591 (JDR)
Koornneef J., 1983, A&A 128, 64
Krolick J.H., Smith H.A., 1981, ApJ 249, 628
Kurucz R.L., 1981, Smithson.Astrophys.Obs., Spec.Rep. 390, 1
Lemaître G., Kolher D., Lacroix D., Meunier J.P., Vin A., 1990, A&A 228, 546
Levreault R.M., 1988, ApJ 330, 897
Lynds B.T., 1962, ApJS 7, 1
Massey P., Strobel K., Barnes J.V., Anderson E., 1988, ApJ 328, 315

Mathis J.S., 1990, ARA&A 28, 37
Mathis J.S., Savage B.D., 1979, ARA&A 17, 73
McGregor P.J., Persson S.E., Cohen J.G., 1984, ApJ 286, 609
Mitskevich A.S., Natta A., Grinin V.P., 1993, ApJ 404, 751
Moore C.E., 1959, A Multiplet Table of Astrophysical Interest, Nat.Bur.Standards, Washington (NBS Technical Note 36)
Morgan L.P., 1971, MNRAS 153,393
Mozurkewich D., Schwartz P.R., Smith H.A., 1986, ApJ 311, 371
Oke J.B., 1974, ApJS 236, 21
Oke J.B., Gunn J.E., 1983, ApJ 266, 713
Osterbrock D.E., Martel A., 1992, PASP 104, 76
Palla F., Stahler S.W., 1990, ApJ 360, L47
Palla F., Stahler S.W., 1991, ApJ 375, 288
Palla F., Stahler S.W., 1992, ApJ 392, 667
Panagia N., 1991, The Physics of Star Formation and Early Stellar Evolution, C.J. Lada & N.D. Kylafis (eds.), NATO ASI Ser., Ser. C, 342, 565
Panagia N., Felli M., 1975 A&A 39, 1
Persson S.E., McGregor P.J., Campbell B., 1988, ApJ 326, 339
Rossano G.S., 1978, AJ 83, 1214
Seidelmann P.K. (ed.), Explanatory Supplement to the Astronomical Almanac, 1992, University Science Books, Mill Valley
Sharpless S., 1959, ApJS 4, 257
Skinner S.L., Brown A., Stewart R.T., 1993, ApJS, in press
Snell R.L., Bally J., 1986, ApJ 303, 683
Snell R.L., Dickman R.L., Huang Y.L., 1990, ApJ 352, 139
Snell R.L., Huang Y.L., Dickman R.L., Claussen M.J., 1988, ApJ 325, 853
Stetson P.B., 1987, PASP 99, 191
Stones R.P.S., 1977, ApJ 218, 767
Tenorio-Taggle G., 1979, A&A 71, 59
Torrelles J.M., Ho P.T.P., Moran J.M., Rodríguez L.F., Cantó J., 1986, ApJ 307, 787

This article was processed by the author using Springer-Verlag LaTeX A&A style file version 3.